AN EFFICIENT KOHONEN-FUZZY NEURAL NETWORK BASED ABNORMAL RETINAL IMAGE CLASSIFICATION SYSTEM

*J. Anitha**, *D. Jude Hemanth**

Abstract: Artificial Neural Network (ANN) is the primary automated AI system preferred for medical applications. Even though ANN possesses multiple advantages, the convergence of the ANN is not always guaranteed for the practical applications. This often results in the local minima problem and ultimately yields inaccurate results. This convergence problem is common among ANNs and especially in Kohonen neural networks which employ unsupervised training methodology. In this work, an Efficient Kohonen Fuzzy Neural (EKFN) network is proposed to eliminate the iteration dependent nature of the conventional system. The suitability of this hybrid automated system is illustrated in the context of pathology identification in retinal images. This disease identification system includes anatomical structure segmentation from retinal images followed by image classification. The performance measures used are accuracy, sensitivity, specificity, positive predictive value and positive likelihood ratio. Experimental results show promising possibilities for the hybrid systems in terms of performance measures.

Key words: *Kohonen neural network, retinal images, fuzzy C-means and accuracy*

Received: April 6, 2011
Revised and accepted: March 11, 2013

1. Introduction

Retinal disease identification is one of the significant applications of the biomedical field. This disease identification process belongs to the category of image classification (pattern recognition) in which different abnormal images are categorized into different groups based on some similarity measures. The accuracy of such abnormality detection system must be exceedingly high since the subsequent treatment planning is dependent on this disease identification system. But, the conventional system of pathology detection is through manual observation which is highly prone

*J. Anitha, D. Jude Hemanth
Department of ECE, Karunya University, Coimbatore, India, E-mail:
{rajivee1@rediffmail.com, jude_hemanth@rediffmail.com}

to error. Hence, automated computer-aided systems are becoming increasingly important for disease identification in human retinal images which are highly accurate than the manual observations.

Different methodologies have been adopted for automated retinal disease identification systems. Usually, most of the automated disease diagnostic systems involve two phases: (a) Anatomical structure detection and (b) Image classification. Initially, anatomical structures are extracted from the images. These extracted features are further used for categorizing abnormal images into different groups. Most of the earlier works are satisfied with the first phase, which is the process of anatomical structures detection such as Optical Disk (OD) detection, blood vessel detection, macula detection, etc. In this work, the research is extended further for image classification which is the process of differentiating different abnormal images based on anatomical structures. The logic behind this approach is that each abnormality affects the anatomical structures in a unique manner. Thus, anatomical features such as OD and blood vessels are detected initially, followed by feature extraction on these segmented structures. These extracted features are further used for automated classification of retinal images based on the abnormalities.

Literature survey reveals the existence of earlier works for abnormal retinal image classification. Several previous researches are independent of intelligence systems and few other approaches are based on AI systems. A prediction image processing algorithm for disease classification is reported in (Raghuraj et al. 2007). This approach is based on the concept of content based image comparison in which there is a necessity for patients previously recorded databases. This shows the requirement for huge memory space which is not practically feasible. No quantitative analysis is provided in this work, which is another drawback of this approach. (Sanchez et al. 2008) have implemented the Linear Discriminant Analysis (LDA) for discriminating the normal images and Diabetic Retinopathy (DR) images. But this approach is tested on a small size database which limits the robustness of the system. A multiscale Amplitude Modulation (AM)-Frequency Modulation (FM) method for differentiating the normal and pathological images is proposed by (Agurto et al. 2010). A new set of features is extracted using the modulation techniques. The classification system used in this approach is based on the histogram of the input image. Four categories of abnormal images are used and comparable classification accuracy is achieved in this work.

Several other researchers depend on AI systems for pathology discrimination in retinal images. Among the AI systems, ANN is widely used for implementation. Back Propagation Neural Network (BPN) based image classification is discussed by (Osareh et al. 2003). A comparative analysis with Support Vector Machines (SVM) is also provided in this report. But the major drawback of this work is its inferior classification accuracy tabulated in this work. Only bi-level classification system is implemented in this paper which is not sufficient to test the ability of the proposed system. Another bi-level image classification system is reported in (Accardo et al. 2003). The normal images and exudates images are differentiated in this work using the BPN network. But the features used in this work are based on the intensity of the input image and not based on the anatomical features. Several previous works have already proved the inefficiency of intensity as a feature for image classification. The application of Multi Layer Perceptron (MLP) for disease identification is explored in (Treigys and Saltenis 2006). But, this methodology suffers from the limitations of lack of robustness and inferior classification accuracy.

Fuzzy ART neural network has been successfully used for DR identification in retinal images (Jayakumari and Santhanam 2007). Lack of quantitative analysis and lack of multi-level classification are the major limitations of this system. Different stages of DR images are differentiated using the BPN network (Yun et al. 2008). The number of features used in this work is much lower, which accounts for the inferior classification accuracy. The features are extracted only from the blood vessels, which is not sufficient for retinal image classification. (Garcia et al. 2009) have used the MLP for disease identification in retinal images. The proposed system is a bi-level classification system used for differentiating the normal and DR images. The features used in this work are mainly intensity based features which do not guarantee high classification accuracy. Color retinal image processing for disease identification is proposed in (Jayanthi et al. 2010). Auto associative neural networks are used for image classification. An extensive feature set is used, which is the major advantage of this approach. Only theoretical aspects are discussed in this work and no emphasis is given to practical implementation. Support Vector Machine based disease diagnosis is implemented and reported in (Osareh et al. 2002). This approach is used for discriminating the different stages of DR. A survey of the different techniques employed in the retinal image classification system is given in (Winder et al. 2009). Few other applications are reported by (Babak et al. 2012 and Zainuddin et al.2012).

The objective of our research work reported in this paper is twofold: (a) Developing an improved image classification system and (b) Developing a performance enhanced ANN for retinal image classification. The drawbacks mentioned in the previous works are eliminated in our approach. The proposed system in this paper is a multi-level classification system in which four categories of abnormal images are used. Also, the features are extracted from the anatomical structures and texture which guarantee high accuracy. In terms of ANN, most of the earlier works have used the conventional ANN and no emphasis is given to performance enhancement of the ANN. In this work, the application of a performance enhanced EKFN network is experimented on retinal image classification. Abnormal retinal images from four different categories are used in this research. Initially, the anatomical structures such as OD and blood vessels are extracted and an extensive set of features is extracted from these structures. These extracted features are further used for ANN based classification systems. Experimental results suggest the superior nature of the proposed EKFN network.

2. Proposed Methodology

An automated system with Artificial Neural Networks is developed for retinal image classification. The framework for the automated system is shown in Fig. 1.

The abnormal retinal images from four different categories are collected from ophthalmologists and used in this work for disease identification system. The raw images are initially processed to enhance the contrast in order to accurately detect the anatomical structures such as OD and vascular network. An extensive set of features is extracted from these anatomical structures which ultimately aid in enhancing the accuracy of the automated image classification system. Two classifiers are used in this work and a comparative analysis is performed among them in terms of the performance measures.

The rest of this paper is organized as follows: Section 3 deals with the retinal image database, and Image pre-processing techniques, Section 4 deals with the OD and blood vessel extraction techniques, Section 5 comprises the feature extraction methodologies, Section 6 deals with the classifiers used for image classification, and Sections 7 and 8 deal with Experimental results and discussions.

3. Retinal Image Database and Image Pre-Processing

The image dataset consists of 420 digital retinal images obtained using the imaging camera. All the images are collected from Lotus Eye Care Hospital, Coimbatore, India. The images are stored as color TIFF images and are 1504×1000 pixels in size for all the objects. The intensity value of all the retinal images ranges from 0 to 255 (for each R, G and B planes). The real time images are collected from four abnormal categories namely Non-Proliferative Diabetic Retinopathy (NPDR), Central Retinal Vein Occlusion (CRVO), Choroidal Neo-Vascularisation Membrane (CNVM) and Central Serous Retinopathy (CSR).

The pre-processing step is a mandatory task in automated image classification system. Pre-processing algorithms are implemented to enhance the original image so that it can increase the chances for success of subsequent processes. In this work, the objective of the pre-processing technique is twofold: (a) Contrast enhancement of the raw image and (b) Converting the original 3-channel image (RGB) to single channel image (G). Literature survey shows that the anatomical

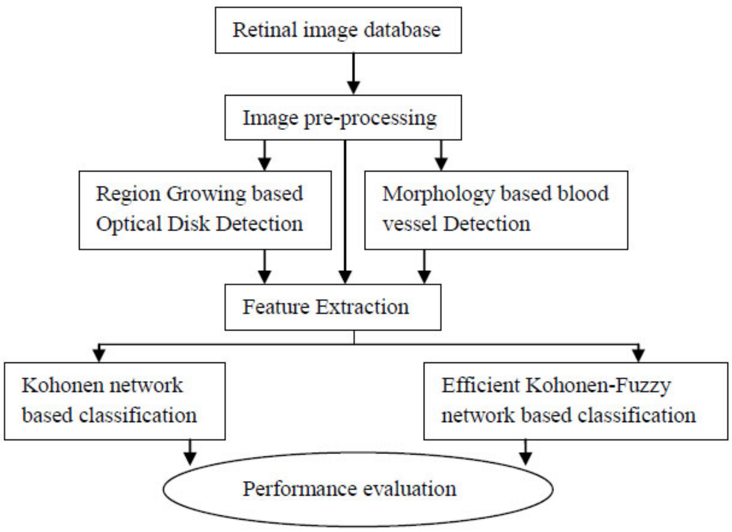

Fig. 1 *Flow diagram of the proposed work.*

structures/background contrast effect is high in the green channel than in the blue and red channels. Again, the subsequent feature extraction process will be made simpler if the single channel image is used. To satisfy these two conditions, the green pixel values are extracted from the input image and stored in the matrix form since it contains more information than the blue channel and the red channel of the image.

The contrast of the retinal images is further improved by histogram equalization which brings out details that are not clearly visible in the green channel image. The resultant image is further enhanced using the Gaussian filter. The second derivative Gaussian filtering is used since it distinguishes the background and foreground region besides enhancing the contrast of the image. Thus, a series of pre-processing methodologies is adopted in this work for image enhancement. After pre-processing, certain anatomical structures are detected from which suitable features are extracted.

4. Anatomical Structure Detection

Anatomical structure detection belongs to the category of image segmentation in which the specific region of interest is extracted from the whole image. The region of interest in this work is the optical disk and the blood vessel network. The main objective of the anatomical structure detection is that these structures represent the nature of the retinal image (type of abnormality). The shape deformation within the OD is an important indicator for the detection of abnormalities such as glaucoma. In particular, the eye care physicians observe the cup-to-disk ratio, sharpness of edge, etc. to diagnose the abnormalities such as retinal occlusion, retinopathy and optical drusen. In the same way, the shape of the vascular network also aids in discriminating the different retinal abnormalities. The effect of pathologies on the vascular network is unique and hence the extracted blood vessels are a useful tool for disease identification. Hence, features such as vessel thickness and vessel orientation can be used for image classification. Thus, it is highly evident that the anatomical structures represent the image in a better way than any other objects.

Most of the previous research works failed to take advantage of this theory. One of the contributions of this work is the exploration of the applicability of anatomical structure based features for retinal disease identification. In this work, the OD is extracted using the region growing technique and the blood vessels are extracted using the morphology based techniques.

4.1 Optical disk detection

Region growing is a simple region-based image segmentation method. It is also classified as a pixel-based image segmentation method since it involves the selection of initial seed points. In this work, the basic seeded region growing method is used. This method takes a set of seeds as input along with the image. The seeds mark each of the objects to be segmented. The regions are iteratively grown by comparing all unallocated neighboring pixels to the regions. The difference between a pixel's intensity value and the region's mean is used as a measure of similarity. The pixel with the smallest difference is allocated to the respective region. This process continues until all pixels are allocated to a region. An elaborative explanation of the algorithm is available in (Ke and Yan 2006; Kose et al. 2008).

4.2 Vascular network detection

Morphological operations (Sopharak et al. 2008) are widely used for extracting the structures which are scattered throughout the image. In this work, a series of morphological operations combined with the thresholding techniques are used to extract the vascular network. The following procedure illustrates the methodology used for vascular network detection.

Step 1: Morphological "opening" operation is performed on the contrast enhanced input image with a "disc" structuring element to filter out the image structures. This process is repeated with different values of radius (10, 15, and 7) for the "disc" structuring element. Initially, different shapes are used in the morphological operation and it has been found that "disc shape" is the optimal shape. Hence, this automated system employs only disc structuring element for opening operation.

Step 2: Adaptive thresholding is performed to binarize the image. Too small a threshold value results in edge linking and a large threshold result in edge segments. Hence, an optimum value of threshold is used, which is 25% of the intensities contained in the image.

5. Feature Extraction

The purpose of feature extraction is to reduce the original data set by measuring certain properties, or features, that distinguish one input pattern from another pattern. The extracted feature should provide the characteristics of the input type to the classifier by considering the description of the relevant properties of the image into a feature space. Nine features are used in this work among which three are based on the extracted blood vessels, three are based on optical disk and the rest are based on the texture of the input image.

5.1 Features based on vascular network

The features such as Tortuosity, Perimeter and Area are extracted from the segmented blood vessels. Since each abnormality affects the blood vessels in a unique manner, these sets of features are found to be highly useful for retinal image pattern recognition applications.

Tortuosity Tortuosity is a property of curve being tortuous (twisted; having many turns). There have been several attempts to quantify this property. The simplest mathematic method to estimate tortuosity is arc-chord ratio: ratio of the length of the curve (L) to the distance between the ends of it (C).

Perimeter The perimeter of an image is estimated by counting the number of perimeter pixels. A pixel is part of the perimeter if it is nonzero and it is connected to at least one zero-valued pixel. The pixel connectivity used is a 4-connected neighborhood.

Area The area of an image is obtained by summing up the areas of each pixel in the image. The area of an individual pixel is determined by looking at its 2-by-2 neighborhood. There are six different patterns, each representing a different area: Patterns with zero on pixels (area = 0) Patterns with one on pixel (area = 1/4) Patterns with two adjacent on pixels (area = 1/2) Patterns with two diagonal on pixels (area = 3/4) Patterns with three on pixels (area = 7/8) Patterns with all four on pixels (area = 1).

5.2 Features based on optical disk

Optical disk is another significant parameter which determines the pathological condition of the retina. Optical disk is usually defined as two concentric circles with the inner circle named as "cup" and the outer circle named as "disk". Initially, the optical disk is segmented using the region growing algorithm and then the following features are extracted from the segmented optical disk.

Disk area It is the number of pixels inside the disk boundary. This value differs for different types of abnormalities.

Cup-to-disk (C/D) area ratio It is the ratio of the number of pixels occupied by the cup region to the number of pixels occupied by the disk region. These measurements are taken in the horizontal direction.

Energy of the optical disk region

$$E = [x(i,j)]^2 \tag{1}$$

It is defined as the squared intensity values of the region covered by the optical disk.

These features aid in differentiating the abnormal image types to a higher extent since these values are sufficiently varying for different abnormal types.

5.3 Features based on texture

The textural features are also used for image classification technique. Textural features such as mean, standard deviation and entropy are extracted from the first order histogram which is estimated from the original input image. These features are computed using the formulae given next.

The first order histogram estimate of $p(b)$ is simply

$$p(b) = \frac{N(b)}{M}, \tag{2}$$

where $b = a$ gray level in the image.
M = total number of pixels in neighborhood window centered about an expected pixel.

$N(b)$ = the number of pixels of gray value b in the same window that $0 \leq b \leq L-1$.

Then, the following measures have been extracted by using first order probability distribution.

Mean

$$S_M = \quad \bar{b} = \sum_{b=0}^{L-1} bp(b) \tag{3}$$

Standard deviation

$$S_D = \sigma_b = \left[\sum_{b=0}^{L-1} \left(b - \bar{b}\right)^2 p\left(b\right)\right]^{1/2} \tag{4}$$

Entropy

$$S_E = -\sum_{b=0}^{L-1} p\left(b\right) \log_2 \left\{p\left(b\right)\right\} \tag{5}$$

Thus, the features which are used for the subsequent ANN based classification are Tortuosity, Perimeter, Area, Disk area, Cup-Disk Area Ratio, Energy, Mean, Standard Deviation and Entropy. The main reasons for selecting these features are: (a) These features work well especially for retinal images. These features are used based on the earlier researches (Narasimha-Iyer et al. 2008; Haralick 1979; Walter et al. 2008), (b) These features yield sufficiently diversified values for different categories which ensure the success of the ANN classification process, (c) Hybrid features selected from textures in combination with anatomical features yield better results, (d) Different abnormalities affect the structure of the blood vessels in a different manner and hence features extracted from these blood vessels such as tortuosity, perimeter and area are included in the feature set and (e) Size of the optical disk varies for different categories and hence features extracted from this optical disk is also included in this work.

6. ANN based Image Classification Techniques

In this technique, two different AI based classifiers are used for pattern recognition. The pattern recognition involves the process of categorizing the different abnormal images based on similarity measures. Among the classifiers used, one is the conventional Kohonen neural classifier and other is the EKFN classifier. The results of the EKFN classifier are compared with the conventional classifier to show the superior nature of the proposed techniques.

6.1 Kohonen neural network based classification

One type of the unsupervised neural networks (Fausett 2004), which posses the self-organizing property, is called Kohonen self-organizing map. Similar to statistical clustering algorithms, these Kohonen networks are able to find the natural groupings from the training data set. As the training algorithm follows the "winner-take-all" principle, these networks are also called as competitive learning networks.

6.1.1 Network design

The topology of the Kohonen self-organizing map is represented as a 2-dimensional, one-layered output neural net. Each input node is connected to each output node. The dimension of the training patterns determines the number of input nodes. During the process of training, the input patterns are fed into the network sequentially. Output nodes represent the 'trained' classes and the center of each class is stored in the connection weights between input and output nodes. The architecture used in this work is 9-4 where the number of input features is 9 and the number of output classes is 4.

6.1.2 Training algorithm

The Kohonen self-organizing map uses the competitive learning rule for training the network. It uses the "winner-take-all" principle in which a winner neuron is selected based on the performance metrics. The weight adjustment is performed only for the winner neuron and the weights of all other neurons remain unchanged. A detailed training algorithm is given below.
Step 1: Initialize weights w_{ij}
Step 2: While stopping condition is false, do steps 3 to 6
Step 3: For each J (output layer neurons), compute

$$D\left(J\right) = \sum_{i} \left(w_{ij} - x_i\right)^2 \tag{6}$$

Step 4: Find index Jsuch that $D\left(J\right)$is a minimum
Step 5: Update the winner neuron's weight using the rule

$$w_{ij}\left(new\right) = w_{ij}\left(old\right) + \alpha\left[x_i - w_{ij}\left(old\right)\right] \tag{7}$$

x_i denotes the intensity values of input data set
α denotes the learning rate.
Step 6: Test for stopping condition (Maximum number of iterations)

Initially, the image dataset is divided into training dataset and testing dataset. The training dataset includes the images from all the four abnormal categories. The above mentioned algorithm is implemented for the training images from the first class and the weight matrices are observed. The same process is repeated for the other three classes and all the four weight matrices are stored for the testing process. Each set of weight matrices corresponds to a class. In the testing process, the distance between the unknown input data and all the four weight matrices are calculated individually. The input data are assigned to the class with the minimum distance value.

In the above algorithm, Step 6 is always a drawback since the convergence condition for training is not clearly framed. Different number of iterations yields different results, which is the major drawback of the conventional Kohonen neural network. This drawback is eliminated in the EKFN which is dealt in detail in the next section.

6.2 Efficient Kohonen Fuzzy Neural (EKFN) network based classification

In this work, an Efficient Kohonen Fuzzy Network (EKFN) is proposed for retinal image classification which is highly efficient since this approach eliminates the iteration dependent nature of the conventional Kohonen neural network. The innovation of this network lies in the methodology of weight estimation which does not require the conventional weight adjustment equations.

6.2.1 Network design

The architecture of the EKFN network is purely neural in nature while the training algorithm involves the concepts of the fuzzy theory. The architecture used for this network is a single layer structure with the number of input layer neurons corresponding to the size of the input feature set, and the number of output layer neurons corresponds to the number of output classes. The architecture used in this work is 9-4. Fig. 2 shows the topology of EKFN network.

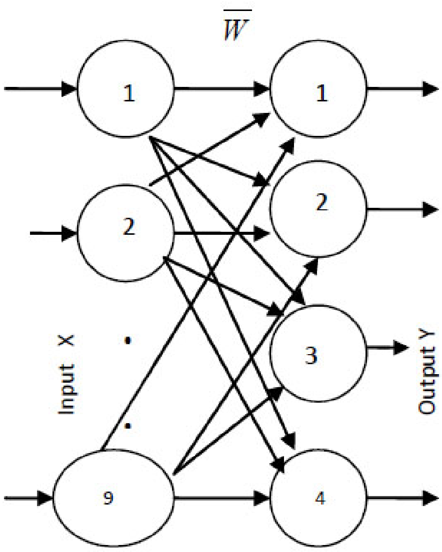

Fig. 2 *Architecture of EKFN network.*

6.2.2 Training algorithm

The training algorithm involves 2 phases: (1) Clustering of training images into different classes using Fuzzy C-means (FCM) algorithm and (2) Assignment of centroid values of the abnormal cluster region to the weight matrix. The following procedure illustrates the algorithm of EKFN.

Phase 1: Clustering using FCM algorithm Fuzzy C-means (FCM) is a method of clustering which allows one pixel to belong to two or more clusters. The FCM algorithm attempts to partition a finite collection of pixels into a collection of "C" fuzzy clusters with respect to some given criterion. Depending on the data and the application, different types of similarity measures may be used to identify classes. Some examples of values that can be used as similarity measures include distance, connectivity, and intensity. In this work, distance is used as the similarity measure. Fuzzy C-means algorithm is based on minimization of the following objective function:

$$J(U, c_1, c_2, \ldots, c_c) = \sum_{i=1}^{c} J_i = \sum_{i=1}^{c}\sum_{j=1}^{n} u_{ij}^m d_{ij}^2 \tag{8}$$

u_{ij} is the membership matrix with values between 0 and 1;
c_i is the centroid of cluster i;
d_{ij} is the Euclidean distance between i_{th} centroid (c_i) and j_{th} data point;
$m \in [1, \infty]$ is a weighting exponent (usually $m = 2$).

Fuzzy partitioning is carried out through an iterative optimization of the objective function shown in Eq. (8), with the update of membership u_{ij} and the cluster centers c_i by:

$$u_{ij} = \frac{1}{\sum_{k=1}^{c}\left(\frac{d_{ij}}{d_{kj}}\right)^{2/(m-1)}}; \quad c_i = \frac{\sum_{j=1}^{n} u_{ij}^m x_j}{\sum_{j=1}^{n} u_{ij}^m}, \tag{9}$$

where x = input feature set.

The entire algorithm can be summarized as follows:
Step 1: Initialize U=[u_{ij}] matrix, U(0)
Step 2: At k_{th} number of iteration:
Calculate the center vectors c_i with u_{ij}

$$c_i = \frac{\sum_{j=1}^{n} u_{ij}^m x_j}{\sum_{j=1}^{n} u_{ij}^m} \tag{10}$$

Step 3: Update the membership matrix U for the k_{th} step and $(k+1)_{th}$ step.

$$u_{ij} = \frac{1}{\sum_{k=1}^{c}\left(\frac{d_{ij}}{d_{kj}}\right)^{2/(m-1)}} \tag{11}$$

Step 4: If || U(k+1) - U(k)|| $< \varepsilon$ then STOP; otherwise return to step 2.

The above algorithm is repeated for all the input training images. The number of clusters for each image used in this work is 4 (background, abnormal region, blood vessels and other anatomical structures). An important constraint of this algorithm is that the number of clusters used in the FCM algorithm must be equal to the number of classes (categories of abnormal images). The output of the FCM algorithm yields the stabilized membership matrices and the centroid values of the four clusters for all the input images. The average centroid values of all images from each category (CSR, CNVM, CRVO and NPDR) are observed for further processing.

Phase 2: Weight estimation through assignment procedure The centroid values obtained for images from the same classes are more similar than the centroid values of the other class images. Thus, the centroid values of the abnormal region are unique for each class which is used as the main base in this technique for image classification. The average centroid values of the training images of the same class are observed, which results in four centroid values for each category. A normalization procedure is used to reduce the dynamic range of the centroid values between 0 and 1. Now, these values are assigned as weight vectors for the neural architecture. As per the architecture, the size of the weight matrix must be 9×4. All the links from the input layer to the first output layer neuron are assigned with the normalized centroid value (C1) of category 1. Similarly, the weight values are assigned for other links. This procedure is illustrated with the following example:

Let

C1, C2, C3, C4 = Average cluster centers of CNVM category images
C5, C6, C7, C8 = Average cluster centers of CRVO category images
C9, C10, C11, C12 = Average cluster centers of CSR category images
C13, C14, C15, C16 = Average cluster centers of NPDR category images

Four set of weight matrices (each of size 9*4) are obtained with each matrices corresponding to a category. The first column of weight matrix of a specified category, say CNVM, are formed with the links ($W_{1,1}$, $W_{2,1} \ldots W_{9,1}$) assigned the values of C1. Similarly, the other links are assigned with cluster centers C2, C3 and C4. The first set of weight matrix is represented as follows:

W1 = [C1 C2 C3 C4
C1 C2 C3 C4
C1 C2 C3 C4
C1 C2 C3 C4
C1 C2 C3 C4
C1 C2 C3 C4
C1 C2 C3 C4
C1 C2 C3 C4
C1 C2 C3 C4]

The matrix W1 is fixed to be the stabilized matrix of the CNVM category. As per the architecture, the size of the stabilized weight matrix must be 9×4. But, the FCM approach yields only 4 cluster center values (background, abnormal region, blood vessels and other anatomical structures) for the input images from each category. To fulfill this dimension requirement, the cluster center value C1 is repeated in the first column for all the rows. Similarly, C2, C3 and C4 are repeated in the 2^{nd}, 3^{rd} and 4^{th} column of the matrix. Thus, the output matrix dimension is now 9×4 and, hence, testing process can be done with this stabilized weight matrix. This process is continued for all the categories and four sets of weight matrices (W1, W2, W3 and W4) are formed at the end of the assignment process. Usually, only one set of weight matrices is obtained for a trained neural network. But, in this approach, four weight matrices are generated with each matrix representing an individual category.

Thus, stabilized sets of weight matrices are obtained without training the neural network. The four sets of weight matrices (W1, W2, W3 and W4) are the stabilized weight matrices which are obtained through the fuzzy based assignment procedure. Using these stabilized weight matrices, the Kohonen neural network is tested with the unknown input data. Thus, the Kohonen neural network is used only for testing. The distance between the input data and the four weight matrices is calculated individually. The input data are assigned to the category for which the distance value is minimum. Since the centroid values depict the characteristics of each abnormal class, they are used to represent each class through the weight matrices. Hence, the weight matrices are estimated without any iterative training methodologies. Even though iterations are involved in FCM algorithm, the number of iterations used for the FCM algorithm is significantly lesser than the number of iterations required for the neural network training procedure.

Thus, an iteration-free Kohonen neural network is developed for image classification which is much efficient than the conventional system. The novelty of this approach is that the fuzzy procedure is used for determining the stabilized set of weight matrices and the Kohonen neural network is used only for testing and not for training the images. The objective of training is to determine the stabilized set of weight matrices which has been already performed by the fuzzy procedure. The testing process is repeated by the Kohonen neural network for all the testing dataset and the overall classification accuracy is estimated.

7. Implementation

To prove the effectiveness of the proposed method, the method is implemented in the real-time dataset provided by Lotus Eye Care Hospital, Coimbatore, India. The dataset used for the classification system is shown in Tab. I.

Class	Training data	Testing data	Number of images per class
CNVM	35	64	99
CRVO	35	60	95
CSR	35	73	108
NPDR	35	83	118
Total abnormal images	420		

Tab. I *Dataset for retinal image classification.*

Several parameters are used in the implementation of this automated system. In case of retinal blood vessel segmentation, the shape of the structuring element used for the "opening" operation is "disk" with a radius value of 10, 15 and 7. The image is subjected to a series of "opening" operations with these radius values. The number of iterations used for the conventional Kohonen neural network training is 2000. The value of learning rate (α) is 0.7. In the EKFN network based system, 4 clusters are used for the FCM based segmentation with an error threshold value of 0.01. The number of iterations used for the FCM algorithm is 200. The software used for the implementation is MATLAB (version 7.0) (Mathworks 2002), developed by Math works Laboratory.

8. Results and Discussions

Experiments are conducted on the retinal image database using the EKFN and the conventional neural classifier (Kohonen network). The performance of these classifiers are analysed based on classification accuracy, sensitivity, specificity, positive predictive value (PPV) and positive likelihood ratio (PLR). These performance measures are defined as follows:

Sensitivity = TP/(TP+FN) (12)
Specificity = TN/(TN+FP) (13)
Accuracy = (TP+TN)/(TP+FP+FN+TN) (14)
PPV = TP/ (TP+FP) (15)
PLR = Sensitivity/ (1-specificity) (16)

In the above expressions, the parameters are defined with an example as follows: TP = True Positive (an image of CNVM type is categorized correctly to the same type), TN = True Negative (an image of Non-CNVM type is categorized as Non-CNVM type), FP = False Positive (an image of Non-CNVM type is categorized wrongly as CNVM type) and FN = False Negative (an image of CNVM type is categorized wrongly as Non-CNVM type). These measures are used to test the efficiency of the system.

After estimating these values for the classifiers, an extensive comparative analysis is made to show the superior nature of the proposed network. Prior to the final image classification technique, the anatomical structure detection procedure and the feature extraction procedure are implemented in the automated system. The results of these implementations are illustrated initially. The rest of the section is organized as follows: (a) Anatomical structure detection results, (b) Feature extraction results and (c) Image classification results.

8.1 Anatomical structure detection results

In this work, two anatomical structures such as optical disk and vascular network are extracted from the retinal image. Since these structures are significantly affected by the abnormalities, these are selected as one of the representatives to distinguish the abnormal images. Region growing technique is used for optical disk detection and morphology approaches are used for vascular network detection. Fig. 3 shows sample segmented images of optical disk and vascular network.

Fig. 3(a) and 3(b) shows the optical disk extracted from two retinal images which are inclined in different directions. A subjective margin is formed around the optical disk to differentiate the "cup" and the "disk" region. Fig. 3(c) and 3(d) shows the vascular network detected using the morphology based operations. "Opening" operation with disk structuring element is used for implementation. After segmentation, an extensive set of features is extracted from these images which are further used for the pattern recognition technique. The segmentation

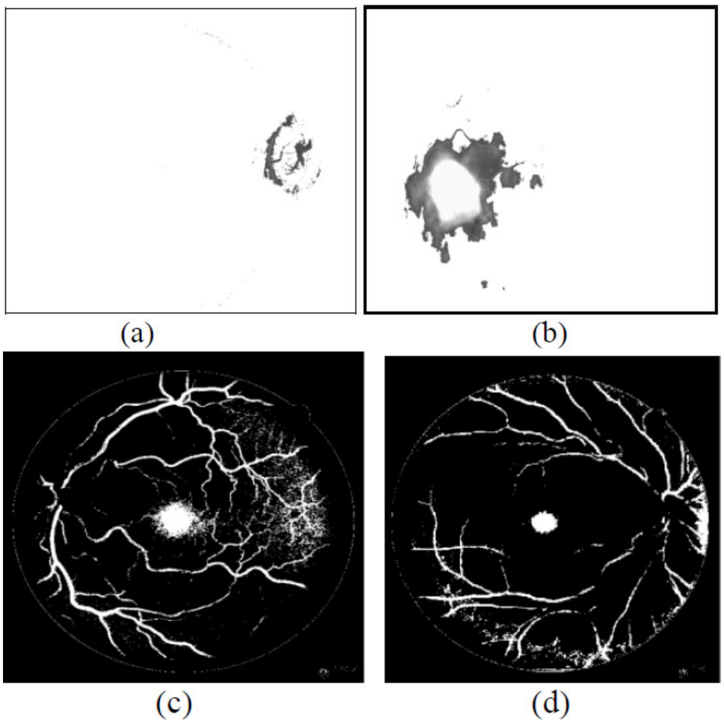

Fig. 3 *Sample segmented images.*

of these structures is sufficiently accurate such that the estimated features are highly diversified for the four abnormal categories. These diversified feature values ultimately aid in improving the accuracy of the neural classifiers.

8.2 Feature extraction results

Three sets of features based on vascular network, optical disk and texture of the original image are extracted and used in this work for image classification. Tortuosity, area and perimeter are based on vascular network; cup-to-disk ratio, cup area and energy are extracted from the optical disk and mean, standard deviation and entropy are extracted from the original input image. A summary of the feature values is reported in this section.

In case of vascular network based features, the values of the area range from 13278±12561 and the values of the perimeter range from $1.23\times10^4\pm\ 2.2\times10^4$. The images with more blood vessels (or) thickened blood vessels such as in the case of CRVO show an increased value for area and perimeter. If the number of twists in the blood vessels is high, then the tortuosity feature value is also high for that image. The size and shape of the anatomical structures are based on the abnormalities and hence the area and perimeter and tortuosity feature values are unique for each class. Even though high segmentation efficiency is not guaranteed, the feature values obtained are sufficient to yield high classification accuracy.

The textural features also yield distinguishable values which are suitable to obtain high classification accuracy. The mean values range from 320±754. Images with abnormalities such as NPDR show a higher value for mean since most of the pixels are white in nature. The value of the standard deviation varies from 34.5± 120. CSR and CNVM images yield a higher standard deviation value since the abnormalities are more distinct, i.e, the difference between two neighboring pixels is significantly high.

The optical disk features yield a sufficiently diversified value for the four categories. All the cup-to-disk ratios are higher than 0.5 [(C/D) > 0.5] with CNVM showing a value of 0.8 and other categories range from 0.6±0.75. The other feature values are also observed which are further used for training the neural classifiers. Thus, the experimental values yield sufficiently accurate feature values for the neural networks to differentiate the different abnormal categories. Hence, it can be claimed that even though the pre-processing and feature extraction procedures are simple, they are sufficient to guarantee the success of the subsequent procedures including the final classification accuracy results.

8.3 Performance measure analysis of the classifiers

The two classifiers are analyzed based on five performance measures to test the effectiveness of the proposed system. Initially, the successful and false classification rates of the classifiers are analyzed individually, followed by the performance measure analysis. The successful and false classification rates are illustrated in the form of confusion matrix. This analysis is performed on the testing images. Tab. II illustrates the misclassification rates of the Kohonen neural network.

	Class 1	Class 2	Class 3	Class 4
CNVM	49	4	6	5
CRVO	3	47	4	6
CSR	6	5	57	5
NPDR	4	7	5	67

Tab. II *Successful and false classification analysis of Kohonen neural network.*

In the above method, 49 images have been successfully classified in CNVM, 47 images have been successfully classified in CRVO, 57 images have been successfully classified in CSR and 67 images have been successfully classified in NPDR. The incorrect weight values due to the irregular convergence conditions lead to the inferior results. Tab. III illustrates the misclassification rates of EKFN network.

In the EKFN technique, 60 images have been successfully classified in CNVM, 57 images have been successfully classified in CRVO, 68 images have been successfully classified in CSR and 77 images have been successfully classified in NPDR. The increase in the correct classification rate is mainly due to the fact that the EKFN is independent of iterations. The performance measure of the classifiers is further analyzed by estimating the TN, TP, FP and FN from the confusion matrices. Tab. IV shows the performance analysis of the conventional Kohonen neural

	Class 1	Class 2	Class 3	Class 4
CNVM	60	1	2	1
CRVO	0	57	2	1
CSR	1	2	68	2
NPDR	1	2	3	77

Tab. III *Successful and false classification analysis of EKFN network.*

	TP	TN	FP	FN	Sensitivity	Specificity	Accuracy(%)	PPV	PLR
CNVM	49	171	13	15	0.76	0.92	88.7	0.79	9.5
CRVO	47	173	16	13	0.78	0.91	88.3	0.74	8.6
CSR	57	163	15	16	0.76	0.91	87.6	0.79	8.4
NPDR	67	153	16	16	0.77	0.90	87.3	0.80	7.7
Overall results					0.77	0.91	88	0.78	8.5

Tab. IV *Performance measures of the conventional Kohonen neural network.*

network. This analysis is initially performed individually on the different classes of images.

Tab. IV shows the inferior nature of the conventional Kohonen neural network in terms of sensitivity and PPV. Both these measures directly impact the TP value which must be significantly high for accurate classification. But, the low values of these measures show the low efficiency of the system. The classification accuracy of this system is also low, which limits the practical application of the conventional Kohonen neural network. These drawbacks are eliminated in the proposed system which is analyzed in Tab. V.

	TP	TN	FP	FN	Sensitivity	Specificity	Accuracy(%)	PPV	PLR
CNVM	60	202	2	4	0.94	0.99	97.7	0.97	94
CRVO	57	205	5	3	0.95	0.98	97	0.92	47.5
CSR	68	194	7	5	0.93	0.97	95.6	0.91	31
NPDR	77	185	4	6	0.93	0.98	96.3	0.95	46.5
Overall results					0.94	0.98	97	0.94	54.8

Tab. V *Performance measures of the EKFN network.*

The sensitivity and the PPV values are sufficiently higher than the conventional system, which proves the efficiency of the system. The PLR value is also higher, which shows the low misclassification rate. A significant increase in classification accuracy is also achieved by the EKFN network over the conventional system. Thus, the efficiency of the EKFN network is verified through the experimental results.

A comparative analysis with the results of other classification methods is shown in Tab. VI. These results are taken from the literature and compared with the proposed method. Only the techniques are highlighted in this comparative analysis and the authors' names are given in square brackets.

Techniques	Sensitivity	Specificity	Accuracy(%)
BPN Neural network [Yun et al.]	0.91	0.98	83
Statistical Classifiers [Niemeijer et al.]	0.85	0.86	-
MLP neural network [Garcia et al.]	0.88	0.85	97
RBF neural network [Garcia et al.]	0.88	0.81	92
SVM [Garcia et al.]	0.87	0.77	91
EKFN network [Proposed Method]	**0.94**	**0.98**	**97**

Tab. VI *Comparative analysis with other approaches.*

The above summary of the previous studies shows the superior nature of the proposed method. Though BPN neural network possesses a higher specificity, the classification accuracy is very low. While the classification accuracy is high in MLP, the sensitivity and specificity values are very low. Thus, the proposed method proves to be much efficient over other systems since it yields optimal results for all the performance measures.

9. Conclusion

In this work, EKFN based automated system is proposed for retinal image classification. This automated system also involves hybrid feature extraction techniques which significantly enhance the efficiency of the proposed neural network. Experiments are conducted on retinal images from four different categories using the proposed method and the results are compared with the conventional Kohonen neural network. An approximate value of 11% increase in accuracy is achieved by the proposed method over the conventional method. A significant increase in other performance measures is also obtained by this EKFN based system. A study with the previous works also confirms the efficiency of the proposed system. Thus, the proposed EKFN network eliminates the practical drawbacks of the conventional Kohonen neural network and proves to be a suitable alternative to the conventional system for real-time applications.

Acknowledgments

The authors thank Dr. A. Indumathy, Opthalmologist, Lotus Eye Care Hospital, India for her guidance in database collection and results validation. The authors also thank Council of Scientific and Industrial Research (CSIR), New Delhi, India for the financial assistance towards this research (Scheme No: 22(0592)/12/EMR-II).

References

[1] RaghuRaj P., Pai K. G., Shylaja S. S.: Algorithmic approach for prediction and early detection of diseases using retinal images. Proceedings of the IEEE International Conference on Computer Graphics, Imaging and Visualisation, 2007, pp. 501-505.

[2] Sanchez C. I. et al.: A novel automatic image processing algorithm for detection of hard exudates based on retinal image analysis. Medical Engineering and Physics, **30**, 3, 2008, pp. 350-357.

[3] Agurto C. et al.: Multiscale AM-FM methods for diabetic retinopathy lesion detection. IEEE Transactions on Medical Imaging, **29**, 2, 2010, pp. 502-512.

[4] Osareh A., Mirmehdi M., Thomas B., Markham R.: Automated identification of diabetic retinal exudates in digital colour images. British Journal of Ophthalmology, 87, 2003, pp. 1220-1223.

[5] Accardo A., Pensiero S.: Neural network based system for early keratoconus detection from corneal topography. Journal of Biomedical Informatics, 35, 2003, pp. 151-159.

[6] Treigys P., Saltenis V.: Neural network as an ophthalmologic disease classifier. Information Technology and Control, **36**, 4, 2006, pp. 365-371.

[7] Jayakumari C., Santhanam T.: Detection of hard exudates for diabetic retinopathy using contextual clustering and fuzzy ART neural network. Asian Journal of Information Technology, **6**, 8, 2007, pp. 842-846.

[8] Yun W. et al.: Identification of different stages of diabetic retinopathy using retinal optical images. Information Sciences, 178, 2008, pp. 106-121.

[9] Garcia M. et al.: Neural network based detection of hard exudates in retinal images. Computer Methods and Programs in Biomedicine, 93, 2009, pp. 9-19.

[10] Jayanthi D., Devi N., Swarna Parvathi S.: Automatic diagnosis of retinal diseases from color retinal images. International Journal of Computer Science and Information Security, **7**, 1, 2010, pp. 234-238.

[11] Osareh A., Mirmehdi M., Thomas B., Markham R.: Comparative exudates classification using support vector machines and neural networks. Proceedings of the 5th International Conference on Medical Image Computing and Computer-Assisted Intervention (MICCAI)-part II, 2002, pp. 413-420.

[12] Winder R. et al.: Algorithms for digital image processing in diabetic retinopathy. Computerized Medical Imaging and Graphics, 33, 2009, pp. 608-622.

[13] Ke H., Yan M.: A region based algorithm for vessel detection in retinal images. Proceedings of Lecture Notes on Computer Science (LNCS), 4190, 2006, pp. 645-653.

[14] Kose C., Sevik U., Gencalioglu O.: Automatic segmentation of age related macular degeneration in retinal fundus images. Computers in Biology and Medicine, 38, 2008, pp. 611-619.

[15] Sopharak A., Uyyanonvara B., Barman S., Williamson H.: Automatic detection of diabetic retinopathy exudates from non-dilated retinal images using mathematical morphology methods. Computerized Medical Imaging and Graphics, 32, 2008, pp. 720-727.

[16] Narasimha-Iyer H. et al.: Automatic Identification of Retinal Arteries and Veins from Dual-Wavelength Images Using Structural and Functional Features. IEEE Transaction on BioMedical Imaging, **54**, 8, 2007, pp. 1427-1444.

[17] Haralick R. M.: Statistical and structural approaches to texture. IEEE Transactions on Systems, Man And Cybernatics, 67, 1979, pp. 786-804.

[18] Walter et al.: Automatic detection of microaneurysms in color fundus images. Medical Image Analysis, 11, 2007, pp. 555-566.

[19] Fausett L.: Fundamentals of Neural Networks: Architectures, Algorithms and Applications. Englewood Cliffs, NJ: Prentice Hall, 2004.

[20] Babak M. A. et al.: An adaptive backpropagation neural network for arrhythmia classification using R-R interval signal. Neural Network World, 22, 2012, pp. 535-548.

[21] Zainuddin Z. et al.: An effective and novel wavelet neural network approach in classifying type 2 diabetics, Neural Network World, 22, 2012, pp. 407-428.

[22] MATLAB, User's Guide, The Math Works, Inc., Natick, MA 01760, 1994-2002.